Revista de metalurgia

Thermal modelling of a torpedo-car(•)

L.F. Verdeja-González*, M.F. Barbés-Fernández*, R. González-Ojeda**, G.A. Castillo*** and R. Colás***

Abstract A two-dimensional finite element model for computing the temperature distribution in a torpedo-car holding pig iron is described in this work. The model determines the temperature gradients in steady and transient conditions within the different parts that constitute the system, which are considered to be the steel casing, refractory lining, liquid iron, slag and air. Heat transfer within the main fluid phases (iron and air) is computed assuming an apparent thermal conductivity term incorporating the contribution from convection and radiation, and it is affected by the dimensions of the vessel. Thermal gradients within the constituents of the torpedo-car are used to calculate heat losses during operation. It was found that the model required the incorporation of a region within the iron-refractory interface to reproduce thermographic data recorded during operation; the heat transfer coefficient of this interface was found to be equal to 30 $Wm^{-2}K^{-1}$.

Keywords Ironmaking. Heat transfer. Refractories. Modelling. Torpedo-car.

Modelización térmica de un carro torpedo

Resumen En este trabajo se describe un modelo bidimensional basado en el método del elemento finito para calcular la distribución de temperaturas en un carro torpedo lleno de arrabio. El modelo determina los gradientes térmicos en condiciones estacionarias y transitorias dentro de las partes que constituyen el sistema considerado, como son cubierta de acero, recubrimientos refractarios, arrabio líquido, escoria y aire. La transferencia de calor en las fases fluidas (arrabio y aire) se calcula suponiendo un coeficiente de conductividad térmica aparente que incorpora las contribuciones por convección y radiación y está afectado por las dimensiones del recipiente. El conocimiento de los gradientes térmicos permite calcular las pérdidas de calor durante la operación del carro. Se encontró que el modelo requiere de la incorporación de una región en la intercara hierro-refractario para reproducir la información termográfica recopilada durante pruebas en planta. El coeficiente de transferencia de calor de esta interacara resultó ser de 30 $Wm^{-2}K^{-1}$.

Palabras clave Siderurgia. Transferencia de calor. Refractarios. Modelización. Carro torpedo.

1. INTRODUCTION

Production of steel from iron ore can be followed by various technological routes, some of them rely in the direct reduction of iron by means of hydrogen, carbon monoxide or any other reducing agent, which is followed by melting the sponge iron formed in electric arc furnaces. However the biggest proportion of steels remains being the blast furnace and basic oxygen furnace route. One of the intermediate stages in this route is the transport of pig iron, produced in the blast furnace, to the basic oxygen furnace, which produce steel. This stage is carried out in specially designed vessels of elongated cylindrical shape known as torpedo-cars [1]. Research work carried out during the last two decades has turned these cars from purely transport and holding vessels to stations in which sulphur, phosphorous and silicon are controlled and eliminated and, due to these, in some steelworks the torpedo-car is called torpedo-ladle [2].

(•) Trabajo recibido el día 8 de noviembre de 2005 y aceptado en su forma final el día 25 de noviembre de 2005.
(*) Cátedra de Siderurgia. E.T.S. de Ingenieros de Minas de Oviedo, España.
(**) Escuela de Ingeniería Industrial. Universidad Panamericana, México.
(***) Facultad de Ingeniería Mecánica y Eléctrica, Universidad Autónoma de Nuevo León, México.

The lining of these vessels is made of different types of layered refractory and insulating materials that can maintain pig iron for more than twenty hours. Turbulence created by pouring and processing iron and slag erode the refractory wall decreasing its thickness and reducing the isolating capacity of the lining [1 and 2], therefore, it is required to evaluate such effect and incorporate it into the thermal behaviour of the vessel.

The aim of this work is to present the results of a finite element model of a torpedo-car. Such a model computes the temperature gradients, within transient and steady state conditions, of the different materials that constitute the system and was implemented with a commercial code. Temperatures at the surface of the vessel were recorded by thermographic means and were used to validate and calibrate the model.

2. MODELLING

The storage capacity of a torpedo-car varies from 150 to 600 t of pig iron. The geometry of the car being modelled is shown in figure 1, the maximum load of this vessel is 245 t, but due to safety reasons, the load is normally limited to 220 t. The dimensions of interest, from the point of view of this work, are shown in table I. For safety reasons, it is required that the thickness of the refractory lining should remain of at least 110 mm, starting from 250 mm, after 180,000 t of pig iron have been transported and processed. The average working cycle of a torpedo-car is of three hours, time that takes to load, desulphurize and unload. The average number of cycles for a car is 818, which means an operational life of 2,454 h for the refractory lining, and an average wear rate of $5.7 \cdot 10^{-2}$ mm/h.

Table I. Dimensions of the torpedo-car

Tabla I. Dimensiones del carro torpedo

Inner area with new refractory.	62 m^2
Steel armour outer surface	100 m^2
Refractory initial thickness (work)	250 mm
Minimum refractory thickness (safety)	50 mm
Total volume	35.5 m^3
Load at 90% volume	220 t

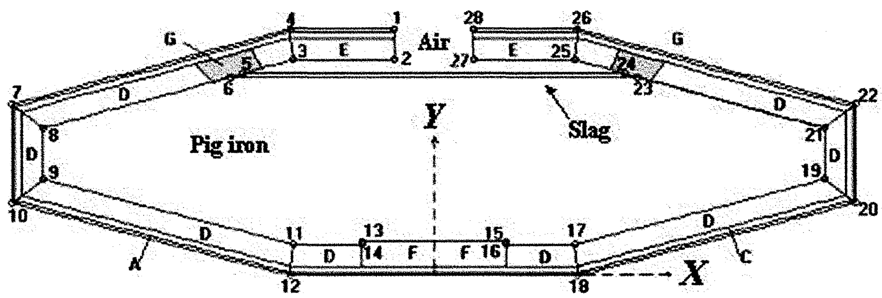

Node	Position X	Position Y	Node	Position X	Position Y
1	-0.55	3.4	15	0.981	0.475
2	-0.55	2.975	16	0.981	0.425
3	-1.925	2.975	17	1.925	0.425
4	-1.975	3.4	18	1.975	0
5	-2.61	2.787	19	5.35	1.325
6	-2.781	2.741	20	5.775	1
7	-5775	2.362	21	5.35	2.037
8	-5.35	2.037	22	5.775	2.362
9	-5.35	1.325	23	2.781	2.741
10	-5.775	1	24	2.61	2.787
11	-1.925	0.425	25	1.925	2.975
12	-1.975	0	26	1.975	3.4
13	-0.981	0.475	27	0.55	2.975
14	-0.981	0.425	28	0.55	3.4

Figure 1. Geometry of the torpedo-car.

Figura 1. Geometría del carro torpedo.

Characteristic values of the thermophysical properties of the various materials used to make torpedo-cars are presented in table II [3-6]. The geometry of the torpedo-car shown in Figure 1 was implemented as a two-dimensional finite element model (FEM) using a commercial code (Cosmos 2.5) to evaluate the thermal behaviour during transient and steady state conditions. The shape of the vessel was constructed with 3,500 triangular elements connected by 2,100 nodes. Figures 2 to 4 show different portions of the geometry. The code assumes that all the constituents of the model are solid, therefore, convection is neglected and conduction is considered to be the solely heat transfer mechanism. The correct simulation of the process requires the incorporation of convection and radiation within the fluid phases (slag, iron and air). These mechanisms are taken into account with the aid of an equivalent conductivity coefficient (k_{eq}) which is implemented by:

$$K_{eq} = h_{c+r} L \qquad (1)$$

where, h_{c+r} represents the contribution from the convective and radiation mechanisms and L represents the lineal characteristic of the system, i.e. k_{eq} vary with the dimensions and coordinates of the system [7]. The model was developed in such a way that an unique term of this equivalent conductivity was required to compute the effect of the slag, as this phase is limited to a thin layer within the model, whereas two different values of k_{eq} were used to compute the gradients along the x and y directions in air and iron, as the vessel is elongated in the x direction, L is bigger along this particular direction. The values of the thermophysical properties used to compute heat

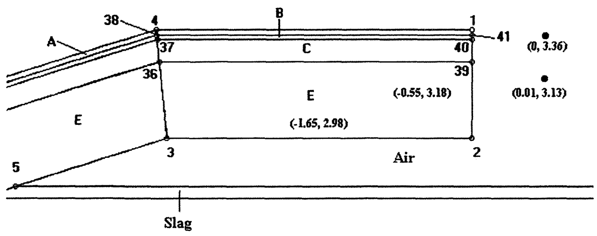

Figure 2. Detail of the upper portion of the torpedo-car.

Figura 2. Detalle de la porción superior del carro torpedo.

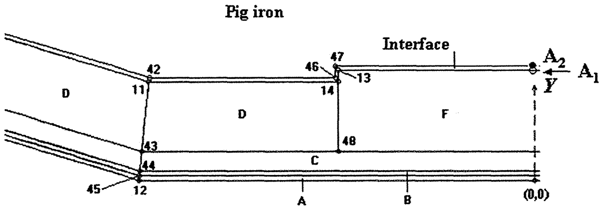

Figure 3. Detail of the bottom portion of the torpedo-car.

Figura 3. Detalle de la base del carro torpedo.

Table II. Thermophysical properties of the materials from which torpedo-cars are made

Tabla II. Propiedades termofísicas de los materiales con los que se fabrican los carros torpedo[3-6]

Material	Density kg m^{-3}	Specific heat J kg^{-1} K^{-1}	Thermal conductivity W m^{-1} K^{-1}
Cover of corrugated steel sheet (A)	7,700	460	50
Expansion joint of polystyrene (B)	1,050	$1.3 \cdot 10^{-3}$	0.12
75%SiO_2 25%Al_2O_3 insulating bricks (C)	1,689	1,068	0.45
8%SiO_2 86%Al_2O_3 refractory brick (D)	2,960	1,047	1.9 (400 °C)
			2.0 (1,000 °C)
13%SiO_2 82%Al_2O_3 refractory brick (E)	2,800	1,054	1.9 (400 °C)
			2.2 (1,000 °C)
38%SiO_2 60%Al_2O_3 refractory brick (F)	2,550	1,076	1.5 (400 °C)
			1.7 (1,000 °C)
6.5%SiO_2 69%Al_2O_3 24.5% SiC refractory brick (G)	2,800	967	6.8 (400 °C)
			4.8 (1,000 °C)

The letters in parenthesis correspond to the various positions in figure 1.

Las letras entre paréntesis corresponden a las diversas posiciones en la figura 1.

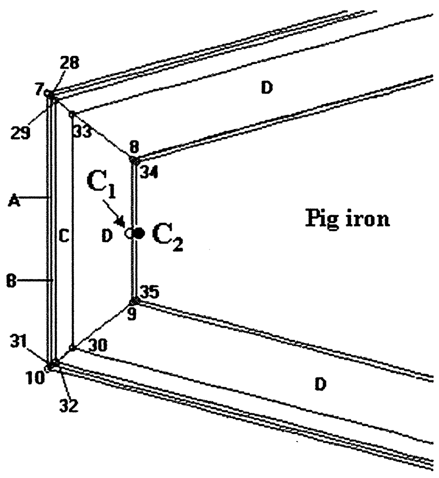

Figure 4. Detail of the left side of the torpedo-car.

Figura 4. Detalle de la porción izquierda del carro torpedo.

transfer within the three fluid phases are shown in table III. The values of k_{eq} reported in this table allow for a difference of no more than 25 °C from the average temperature, within any node considered to be made of iron, and of 896 °C at position (0, 3.36) and 1,071 °C at position (0.01, 3.13) in figure 2, which are occupied by air.

It can be seen in figure 1 and table II that four different types of refractory bricks (identified as D, E, F and G) and one layer of insulating bricks (C) are used for modelling the lining of the torpedo car. In practice, the refractory lining of a torpedo car is usually made of two layers. The deepest one is made of 50 mm thick safety refractory (normally 60 % SiO_2-40 % Al_2O_3), whereas the layer in contact with pig iron is the one described in table I. This layer is kept to a thickness of around 250 mm due to economical reasons. The practical aspect in modelling these two refractory layers can be dealt by using the thermophysical values shown in table II for a 300 mm thick layer, as it is considered that the 20 mm thick polystyrene expansion joint (B in figure 2 and table II) that holds the bricks compensates the effect of the safety refractory.

Table III. Thermophysical properties of the fluid phases within the torpedo-car

Tabla III. Propiedades termofísicas de las fases fluidas dentro del carro torpedo [3-6]

Material	Density kg m^{-3}	Specific heat J kg^{-1} K^{-1}	Thermal conductivity W m^{-1} K^{-1}
Slag	2,767	1,520	0.30
Pig iron	8,249-0.93·T	1,000-0.808·T+5.651·T^2	930 (**x**)
			310 (**y**)
Air	1.1	1,520	6.0 (**x**)
			3.0 (**y**)

Temperature (*T*) in the pig iron is in Celsius (ºC); *x* and *y* indicates the different values of k_{eq}.

La temperatura (*T*) en el arrabio es en ºC; x e y indicn los diferentes valores de k_{eq}.

The area subjected to most damage in the torpedo car is the mouth. The refractory used is made of a composite material made of a stainless steel mesh that supports a ceramic matrix. But, as the thermal contribution of this region is considered to be small, when comparing the total body of the vessel, it was decided to neglect this material and assume that the mouth is made of the refractory identified as E in table II, see figures 1 and 2. The mouth is covered by a ceramic blanket, held with a steel plate, during transport.

The practice in site consist that of loading the vessel with pig iron while the car is hot, to minimize the damage to the lining. In such case, the steady state will be reached in few minutes. Such state is characterized by heat transfer by convection and radiation to the surrounding media through the steel cover, and by the heat flux associated with the maximum temperature reached while pouring the iron.

Heat transfer to the surrounding media is computed with the use of an equivalent heat transfer coefficient (h_q) given by:

$$h_q = h_c + h_r \qquad (2)$$

where, h_c and h_r are respectively the coefficients for convection and radiation. It is considered that h_q depends on the orientation of the steel surface. Table IV shows the values used after assuming that ambient temperature is 15 °C. The values associated with the horizontal surfaces, top and bottom respectively, are identified as OY^+ and OY, as it considered that heat flows in the vertical direction in the positive (top) and negative (bottom) sense. The value used in either vertical wall is identified as $OX^{+/-}$. The conditions for the mouth of the vessel are computed by assuming that the surface area has an equivalent heat transfer coefficient (h_q) of 12 $Wm^{-2}K^{-1}$ [7].

The steady state solution of the heat transfer problem requires a heat source being imposed. In the present case, a temperature of 1,470 °C was

Table IV. Values of the equivalent heat transfer coefficient in equation (2)

Tabla IV. Valores de los coeficientes de transferencia de calor equivalentes en la ecuación (2)

Relative position of the steel surface	h_q (Wm^2K^{-1})
Top horizontal surface (OY^+)	17.9
Bottom horizontal surface (OY^-)	15.8
Vertical surfaces ($OX^{+/-}$)	14.0

assumed at the slag-pig iron interface (from node 6 to node 23 in figure 1). This temperature is calculated after assuming that the working temperature of the blast furnace crucible is 1,500 °C; it is normal practice during bleeding to take three measurements of the fluid iron, one at the start, the second at mid-bleeding, and the last one just before closing the tap hole. The last one is the highest and relates very closely with the working temperature of the crucible[8-10].

Pig iron looses heat while the vessel is being filled, and this can be attributed to radiation from the stream being poured in air, and to the flow to the vessel. The stream of liquid iron gets in contact with air in a similar way to that shown in figure 5 that shows pouring into a ladle. Heat losses can be calculated taking into account that[11]:

- heat losses are controlled by radiation, a 0.4 coefficient for the emissivity (ε) is used,
- the surrounding area of the stream is 3 m^2 (3.75 m long by a 0.8 m perimeter),
- filling time is 20 minutes;

in such a case:

$$Q_r = (3)\varepsilon\sigma(1748^4 - 288^4) = 6{\cdot}35{\cdot}10^5\ W \qquad (3)$$

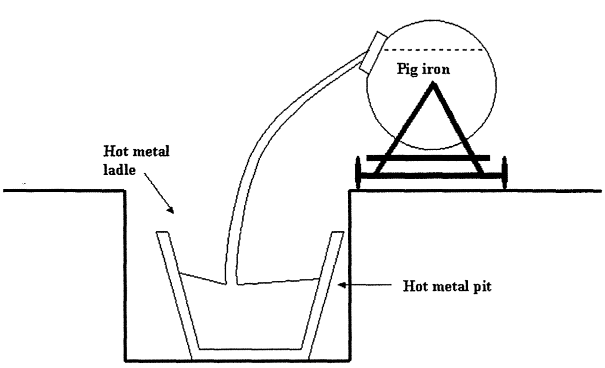

Figure 5. Schematic diagram of pig iron being poured in a ladle.

Figura 5. Diagrama esquemático del arrabio siendo vaciado en una cuchara.

where, Q_r is the heat lost by radiation, and the value for the Stefan-Boltzmann constant (σ) is equal to $5.67{\cdot}10^{-8}$ W/m^2K^4.

The temperature lost during this period of time ($\Delta T/\Delta t$) can be computed by:

$$\frac{\Delta T}{\Delta t} = \frac{Q_r}{m \cdot c_p} = \frac{6 \cdot 35 \cdot 10^5}{22 \cdot 10^5 \cdot 831} = 3 \cdot 47 \cdot 10^{-3}\ K/s \qquad (4)$$

where, a value of 831 J $kg^{-1}K^{-1}$ was taken for the heat capacity of pig iron. With the values of equation (4), a reduction of around 4 °C is found for 20 min pouring.

In a similar way, the heat lost by the iron while flowing within the casthouse before being poured into the vessel can be computed taking into account the following hypothesis[11]:

- heat losses are due to radiation, of which 50% are recovered by radiation shields or absorbed by the slag,
- the emissivity of the hot metal is equal to 0.4,
- the surface area of the stream is 37.5 m^2 (50 m long by a 0.75 m perimeter);
- the time of transit is 20 min;

which yields to:

$$Q_r = (37{\cdot}5)\ (0{\cdot}5)\varepsilon\sigma(1748^4 - 288^4) = 3{\cdot}97{\cdot}10^6\ W \quad (5)$$

The temperature lost during this period of time is computed by:

$$\frac{\Delta T}{\Delta t} = \frac{3 \cdot 97 \cdot 10^6}{22 \cdot 10^5 \cdot 831} = 2 \cdot 17 \cdot 10^{-2}\ K/s \qquad (6)$$

which yields to a decrease of around 26 °C for the 20 min period.

3. RESULTS AND DISCUSSION

The thermal distribution obtained by modelling was validated with thermographic data obtained on site. These data indicate that the temperature on the steel cover varied in the 100 to 200 °C range. It was not possible to insert thermocouples into the car as the trials were made in a vessel that can reach a speed of up to 80 km/h while transporting pig iron from the blast furnace to the oxygen converters. Furthermore, the insertion of thermocouples will have to be made by drilling in cold vessels, which will alter operational conditions and may damage the refractory lining, and, with it, the operational life of the torpedo-car will be reduced.

It was required to incorporate a new 20 mm layer on the periphery of the refractory that will be in contact with the iron to obtain a good correlation between the thermographic values and the results of the model. Different nodes were placed in this region to conduct the analysis. Fig. 6 shows the variation in temperature in four of these nodes as a function of the thermal conductivity assigned to this new layer. The nodes identified as A_1 and A_2 in figure 6 were located at mid-length bottom of the vessel, see figure 3. A_1 is located directly in the region subjected to the impact of iron while poured, whereas A_2 is placed 20 mm below A_1. The positions of nodes C_1 and C_2 are indicated in figure 4; C_1 is at mid-height of the car in contact with the iron and C_2 is located 20 mm inside the layer. A good agreement between the temperatures predicted on the surface of the steel casing and those measured by thermographic means was obtained when the thermal conductivity of this particular region was close to 0.6 $Wm^{-1}K^{-1}$, which yields an apparent heat transfer coefficient of 30 $Wm^{-2}K^{-1}$ between iron and refractory.

The model can be used to analyze the changes in temperature within the iron as a function of time. Figure 7 shows the temperature distribution, given by the value reached by each individual node, at the end of pouring (which can be considered as time zero). The model indicates that the temperature decreases with time, figure 8 and table V.

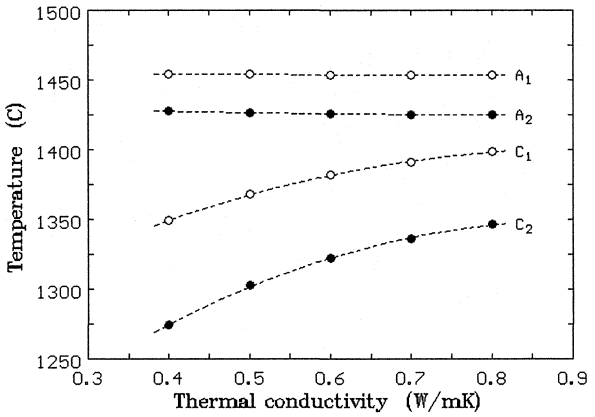

Figure 6. Changes in temperature at the four nodes shown in figures. 3 and 4 as a function of thermal conductivity of the region in which they are located.

Figura 6. Cambio de temperatura en los cuatro nodos indicados en las Figures. 3 y 4 en función de la conductividad térmica de la región en que se localizan.

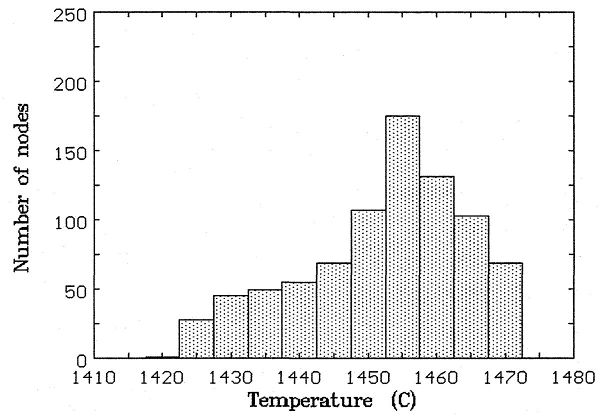

Figure 7. Temperature distribution within the pig iron at the end of filling.

Figura 7. Distribución de temperatura en el arrabio al término del llenado.

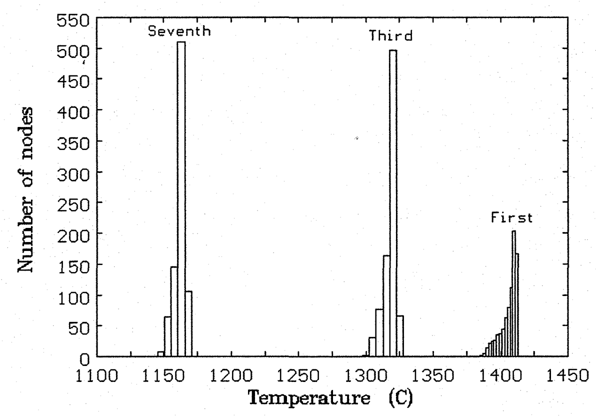

Figure 8. Temperature distribution within the pig iron after the 1st, 3rd, and 7th days.

Figura 8. Distribución de temperatura en el arrabio después del 1er, 3er y 7º días.

Table V. Statistical data of the temperatures of the pig iron

Tabla V. Datos estadísticos relativos a las temperaturas del arrabio

Condition	Temperature (C)	
	Average	Standard deviation
After filling	1,452.2	11.9
First day	1,406.1	6.0
Third day	1,317.9	4.5
Seventh day	1,161.9	4.0

Computer simulation allows the understanding of situations that are difficult to visualize. For instance, the results shown in figure 8 indicate that the pig iron can stay in a liquid state for one week assuming that the integrity of the refractory is maintained, i.e. it is not subjected to either mechanical or chemical wear, and that the metal is poured at an adequate temperature, ranging within the 1,420 to 1,470 °C interval. In the other hand, when bleeding at temperatures ranging between 1,250 and 1,300 °C (that are associated with difficulties in slag removal), the eutectic temperature of the Fe-C system (1,147 °C) will be reached in less than two days.

The model also allows the evaluation of different phenomena taking place within the refractory lining, for instance, the removal of the isolating layer identified as C in figures 2 to 4 and table II has been becoming a common practice to reduce costs and saving time in the installation of the refractory lining. Results from the model indicate that the elimination of such a layer yields to an increase of 50 °C at the surface of the steel armour.

4. CONCLUSIONS

A finite element model that is able to compute the thermal distribution within a torpedo-car was elaborated using a commercial code. Heat transfer conditions within iron and air were modified to allow for an equivalent thermal conductivity term that incorporates the effects of conduction, convection and radiation, as the code is only able to compute conduction.

A good agreement between thermographic data obtained on site and the predictions of the model was achieved once a layer of 20 mm in thickness was placed at the periphery of the refractory that acts as interface with the pig iron. The thermal conductivity of this region was equal to 0.6 $Wm^{-1}K^{-1}$, which yields to an apparent heat transfer coefficient of 30 $Wm^{-2}K^{-1}$ between iron and refractory.

The model indicates that the temperature range is reduced with time. Results from the model were used to explain the behaviour observed during operation.

Acknowledgements

The authors acknowledge the support from the Spanish Ministry of Science and Technology (MAT2003-00502), The International Affairs Directorate of the University of Oviedo, Aceralia, Acelor Steelwork Corporation, the Mexican National Council for Science and Technology (*CONACYT*), and the Program for the Support of Scientific and Technological Research of UANL (*PAICYT*) for the support provided to this work.

REFERENCES

[1] J. SANCHO, L.F. VERDEJA AND A. BALLESTER, *Metalurgia Extractiva. Vol. II*, Madrid, 2000, pp. 56-79.

[2] Y. TAKAMIYA, Y. ENDO AND S. HOSOKAWA, *Refractories Handbook*, Technical Association of Refractories, Japan (TARJ), Torpedo Ladles, 1998, pp. 372-375.

[3] *Ceramic Source*, American Ceramic Society Vol. 8, TD72-TD76, Westerville, 1992.

[4] O. KNACKE, O. KUBASCHEWSKI AND K. HESSELMANN, *Thermochemical Properties of Inorganic Sustances*, Springer-Verlag, 2th Ed., Berlín, 1991.

[5] D.R. POIRIER AND G.H. GEIGER, *Transport Phenomena in Materials Processing*, TMS, Warrendale, 1994.

[6] L.H. VAN VLACK, *Elements of Materials Science and Engineering*, Addison–Wesley 6th Ed, Cambridge, 1989.

[7] D.R. POIRRIER AND F.J. POIRRIER, *Heat Transfer Fundamentals for Metal Casting*, TMS, Warrendale, 1992.

[8] M.A. ROMERO, J. JIMÉNEZ, J. MOCHÓN, J.L. MENÉNDEZ, A. FORMOSO AND F. BUENO, *Rev. Metal. Madrid* 36 (2000) 40-46.

[9] L.F. VERDEJA, R. GONZÁLEZ, A. ALFONSO AND M.F. BARBÉS, *Rev. Metal. Madrid* 39 (2003) 183-192.

[10] H.W. GUDENAU, D. SENK, K. FUKADA, A. BABICH, C. FROEHLING, L.L. GARCÍA, A. FORMOSO, F.J. ALGUACIL AND A. CORES, *Rev. Metal. Madrid* 39 (2003) 367-377.

[11] R.I.L. GUTHRIE, *Engineering in Process Melallurgy*, Oxford Science Publications, Oxford, 1993, pp. 231-233.